Universality in surface growth: Scaling functions and amplitude ratios

Jacques G. Amar and Fereydoon Family
Department of Physics, Emory University, Atlanta, Georgia 30322
(Received 22 October 1991)

A scaling analysis of a variety of nonlinear equations for surface growth is presented. It predicts the existence of universal scaling functions and amplitude ratios for the surface width $w(L,t)$ on length scale L at time t and for the height-difference correlation function $G(\mathbf{x},t)$. This analysis is applied to the Kardar-Parisi-Zhang (KPZ) equation for driven interface growth in $d=2$, in order to derive explicit scaling forms for the amplitudes associated with the scaling of the surface width, correlation function, and saturation velocity as a function of the hydrodynamical parameters in the KPZ equation. A mode-coupling calculation that estimates the values of the various universal amplitude ratios, as well as the associated universal scaling functions is also presented. Our predictions are confirmed by simulations of three different surface-growth models in $d=2$ from which the amplitude ratios as well as the universal scaling function for the surface width $w(L,t)$ (for the case of periodic boundary conditions) are numerically determined. These results are also supported by numerical integration of the KPZ equation in $d=2$. The universality of the height-fluctuation distribution function is also discussed. Our scaling analysis is expected to be useful in the analysis of experiments and in the study of a variety of models of surface growth as well as in establishing a more detailed connection between continuum surface-growth equations and microscopic models.

PACS number(s): 05.40.+j, 64.60.Ht, 68.55.−a, 68.10.Jy

I. INTRODUCTION

Rough surfaces and interfaces are found in a wide variety of natural and industrial processes. Recently, there has been considerable effort in understanding the dynamics of growing surfaces [1]. Much of this interest and activity is based on the recognition that surface fluctuations exhibit scaling behavior in both time and space. In particular, assuming an initially flat interface, the scaling of the interface width is expected to be of the form [2],

$$w(L,t)=L^{\alpha}f(t/L^{z}) , \tag{1}$$

where $w(L,t)$ is the interface width on length scale L at time t, $z=\alpha/\beta$ is the dynamic exponent, and the scaling function $f(x)\sim x^{\beta}$ for $x\ll 1$ and $f(x)\rightarrow$const for $x\gg 1$. A phenomenological equation that applies to a large class of surface-growth models in the hydrodynamic (long-wavelength) limit has been proposed [3] by Kardar, Parisi, and Zhang (KPZ). It is a nonlinear equation for the time dependence of the interface height $h(\mathbf{x},t)$ in a d-dimensional system, above a $(d-1)$-dimensional plane,

$$\frac{\partial h}{\partial t}=\nu\nabla^{2}h+(\lambda/2)(\nabla h)^{2}+\eta(\mathbf{x},t) , \tag{2}$$

where the noise $\eta(\mathbf{x},t)$ satisfies

$$\langle \eta(\mathbf{x},t)\eta(\mathbf{x}',t')\rangle=2D\delta^{d-1}(\mathbf{x}-\mathbf{x}')\delta(t-t') .$$

In $d=2$ the scaling exponents for the KPZ equation ($\lambda\neq 0$) have been found from a renormalization-group analysis [3,4] to be $\alpha=\frac{1}{2}$, $\beta=\frac{1}{3}$, $z=\frac{3}{2}$. For $\lambda=0$ one has Edwards-Wilkinson [5] behavior for which $\alpha=\frac{1}{2}$, $\beta=\frac{1}{4}$, $z=2$ in $d=2$.

The study of a variety of microscopic models [2,6–9] agrees with the renormalization-group predictions for the exponents in $d=2$. However, there has been no rigorous demonstration of the relation between the KPZ equation and these discrete models [10,11]. In addition, most of the attention has centered on the asymptotic exponents, while less attention has been given to the connection between models of surface growth and the corresponding continuum equations. Thus, a more detailed study of the scaling behavior of the KPZ equation would be helpful in establishing a connection between the discrete models and the continuum description.

In this paper we derive expressions for the scaling behavior of the asymptotic coefficients C_t [$C_t=w(\infty,t)/t^{1/3}$] and C_L [$C_L=w(L,\infty)/L^{1/2}$] as a function of the hydrodynamic parameters λ, D, and ν from the scaling properties of the KPZ equation in $d=2$. From these expressions the ratio D/ν (up to a universal constant u_L) as well as the coefficient λ may be obtained directly. Our scaling analysis also predicts the existence of a universal scaling function as well as universal amplitude ratios for the KPZ equation in $d=2$. A similar scaling analysis is also used to predict universal amplitude ratios (and scaling functions) for several other surface-growth equations. In addition, we present the details of a mode-coupling-approximation calculation, based on the renormalization-group equations for the KPZ equation in $d=2$, which further supports our scaling arguments. From this analysis, approximate values of the amplitude ratios and scaling function are predicted. Simulations of discrete models as well as the results of direct numerical integration of the KPZ equation are also presented in order to test our scaling and mode-coupling predictions. A shorter discussion of these results was previously given in

 ©1992 The American Physical Society

Ref. [12]. Below is a more detailed outline of the paper.

In Sec. II we discuss the application of scaling arguments to derive universal scaling relations for the surface width $w(L,t)$ and the correlation function $G(x,t)$ in terms of the equation parameters for general surface-growth equations. We then apply these arguments to the KPZ equation in $d\neq 3$ as well as make specific predictions in $d=2$. The special case of $d=3$ is discussed separately and compared with the work by Tang, Nattermann, and Forrest [13]. As an illustration, we also apply general scaling arguments to predict universal scaling relations for two other nonlinear growth models, the conserved surface-growth model of Sun, Guo, and Grant [14], and the nonlinear molecular-beam-epitaxy (MBE) model of Lai and Das Sarma [15]. The rest of the paper is devoted to the special case of the KPZ equation in $d=2$. In Sec. III we present the details of a mode-coupling-approximation calculation, which supports our scaling analysis for this case. Using the first-order renormalization equations and a mode-coupling approximation, the amplitude ratio R and the universal scaling function $F(x)$ for the KPZ equation in $d=2$ are estimated. Similar results for the correlation function $G(x,t)$ are also derived. In Sec. IV we present the results of simulations of three different surface-growth models in the KPZ universality class which we used to test our predictions. Good agreement with the scaling predictions as well as the mode-coupling-approximation predictions for the universal amplitude ratio R and universal scaling function is obtained. A comparison of our mode-coupling predictions for the asymptotic behavior of the correlation function $G(x,t)$ with simulations of the single-step model is also presented. In addition, results from numerical integration of the KPZ equation in $d=2$ are presented and compared with our scaling predictions. Finally, in Sec. V, we give a summary and discussion of our results. The Appendix presents the derivation of the appropriate growth formulas for the surface width $w(L,t)$ and correlation function $G(x,t)$ in the linear ($\lambda=0$) case, which are used as a starting point for Sec. III.

II. SCALING ANALYSIS OF SURFACE-GROWTH EQUATIONS

The scaling analysis of a nonlinear continuum equation for surface growth may be performed as follows. We consider a scale transformation from the original variables $\mathbf{x},h,t$ to new variables $\mathbf{x}',h',t'$ of the form

$$h=ah' , \tag{3a}$$

$$\mathbf{x}=b\mathbf{x}' , \tag{3b}$$

$$t=ct' , \tag{3c}$$

where a, b, and c are chosen so that the parameters in the transformed equation for h' are now constants typically equal to 1. Consequently, the new variables will in general be *dimensionless.* (For example, in the case of the KPZ equation, we will use the transformation, $\nu\rightarrow\nu'=1$, $2D\rightarrow 2D'=1$, $\lambda/2\rightarrow\lambda'/2=1$.) We note that such a transformation may not always be possible.

If we now assume that the transformed equation has the solution $w'(L',t')=g(L',t')$, we may transform back to obtain the generalized solution for $w(L,t)$,

$$w(L,t)=a\,g(L/b,t/c) . \tag{4}$$

Similarly, if we assume that the scaled equation satisfies the scaling relation $w'(L',t')=L'^{\alpha}f(t'/L'^{z})$, then transforming back, we obtain the asymptotic scaling form

$$w(L,t)=(a/b^{\alpha})L^{\alpha}f((b^{z}/c)t/L^{z}) , \tag{5}$$

where $f(x)$ is a universal scaling function for each growth model.

Similar expressions may be written for the correlation function $G(x,t)=\langle[\tilde{h}(x'+x,t'+t)-\tilde{h}(x',t')]^2\rangle$, where $\tilde{h}(x,t)=h(x,t)-\langle h(x,t)\rangle_x$. Assuming that $G(x,t)$ (at saturation or $t'\gg L^{z}$) satisfies the scaling form $G(x,t)\sim x^{2\alpha}f_G(t/x^{z})$, we may write

$$G(x,t)=(a^2/b^{2\alpha})x^{2\alpha}f_G((b^{z}/c)t/x^{z}) , \tag{6}$$

where $f_G(0)=1$ and $f_G(u)=g_t u^{2\beta}$ for $u\gg 1$. We now discuss the application of this type of scaling analysis to several different growth models.

A. KPZ equation in d dimensions

In the case of the KPZ equation [Eq. (2)] we would like to transform to new variables $\mathbf{x}',h',t'$ so that

$$\frac{\partial h'}{\partial t'}=\nabla'^{2}h'+|\nabla' h'|^2+\xi(\mathbf{x}',t') \tag{7}$$

where

$$\langle\xi(\mathbf{x}'_1,t'_1)\xi(\mathbf{x}'_2,t'_2)\rangle=\delta^{(d-1)}(\mathbf{x}'_1-\mathbf{x}'_2)\delta(t'_1-t'_2)$$

so that $\nu\rightarrow\nu'=1$, $\lambda/2\rightarrow\lambda'/2=1$, and $2D\rightarrow 2D'=1$. Performing the transformation, we obtain the following three conditions on a, b, and c:

$$\nu'=1=\nu c/b^2 , \tag{8a}$$

$$\lambda'/2=1=\lambda ac/2b^2 , \tag{8b}$$

$$2D'=1=2Dc/a^2b^{d-1} . \tag{8c}$$

Solving, we obtain

$$a=2\nu/\lambda , \tag{9a}$$

$$b=(\nu^3/\lambda^2 D)^{1/(3-d)} , \tag{9b}$$

$$c=(\nu^{(3+d)}/\lambda^4 D^2)^{1/(3-d)} . \tag{9c}$$

In $d=3$, the transformation blows up, so clearly (9) is only valid for $d\neq 3$. Assuming this scaling analysis continues to be applicable in $d>3$, we may substitute (9) into (5), using the scaling relation [7,16] $z=2-\alpha$, to obtain the asymptotic scaling form

$$w(L,t)=(|\lambda|^{2\alpha+d-3}D^{\alpha}/\nu^{3\alpha+d-3})^{1/(3-d)}L^{\alpha}\times f((|\lambda|^{2\alpha}D^{\alpha}/\nu^{3\alpha+d-3})^{1/(3-d)}t/L^{z}) , \tag{10}$$

where f is a universal scaling function characteristic of the KPZ equation, which satisfies $f(u)=u_t u^{\beta}$ for $u\ll 1$ and $f(\infty)=u_L$. Defining $C_L=w(L,\infty)/L^{\alpha}$, (10) may be rewritten as

$$w(L,t)=C_L L^{\alpha} F(|\lambda| C_L t/L^z) , \quad (11)$$

where $F(x)=(1/u_L)f(x/u_L)$. From the definition of $F(x)$, $F(\infty)=1$, and $F(u)=u_t/u_L^{\beta+1}$ for $u \ll 1$, so that Eq. (11) implies, using the relation $\beta=\alpha/z$,

$$w(\infty,t)=(u_t/u_L^{\beta+1}) C_L^{\beta+1}|\lambda|^{\beta} t^{\beta}=C_t t^{\beta} . \quad (12)$$

This implies the existence of a universal amplitude ratio,

$$R=C_t/(|\lambda|^{\beta} C_L^{\beta+1})=u_t/u_L^{\beta+1} , \quad (13)$$

where $C_t=w(\infty,t)/t^{\beta}$ and $C_L=w(L/\infty)/L^{\alpha}$.

Similarly, using (6) we can also write for the correlation function,

$$G(x,t)=(|\lambda|^{2\alpha+d-3} D^{\alpha}/\nu^{3\alpha+d-3})^{2/(3-d)} x^{2\alpha} \times f_G((|\lambda|^{2\alpha} D^{\alpha}/\nu^{3\alpha+d-3})^{1/(3-d)} t/x^z) , \quad (14)$$

where f_G is a universal function satisfying $f_G(0)=g_x$ and $f_G(u)=g_t u^{2\beta}$ for $u \gg 1$. Here x corresponds to a particular direction along the $(d-1)$-dimensional substrate. Taking $A_x=G(x,0)/x^{2\alpha}$ and defining $F_G(u)=(1/g_x) f_G(u/g_x)$, this may be rewritten in the form

$$G(x,t)=A_x x^{2\alpha} F_G(|\lambda| \sqrt{A_x} t/x^z) , \quad (15)$$

where $F_G(0)=1$ and $F_G(u)=(g_t/g_x^{2\beta+1}) u^{2\beta}$ for $u \gg 1$. Equation (15) implies $G(0,t)=(g_t/g_x^{2\beta+1}) A_x^{\beta+1} \lambda^{2\beta} t^{2\beta}$, yielding an additional universal amplitude ratio,

$$R_G=A_t/(|\lambda|^{2\beta} A_x^{\beta+1})=g_t/g_x^{2\beta+1} , \quad (16)$$

where $A_t=G(0,t)/t^{2\beta}$ and $A_x=G(x,0)/x^{2\alpha}$.

We note that for $d>3$ there exists a transition [3,16,17] from strong-coupling exponents to weak-coupling exponents (flat phase) as a function of the nonlinear coupling parameter. In that case there could exist a dependence on a cutoff length in addition to the macroscopic parameters λ, D, and ν, so that even in the strong-coupling regime, the above scaling analysis may not hold. However, for completeness we have presented our scaling analysis in general dimensions. In what follows, we focus on $d=2$ and $d=3$ where this problem does not occur.

B. KPZ equation in $d=2$

In two dimensions, Eqs. (9a)–(9c) become

$$a=2\nu/\lambda , \quad (17a)$$

$$b=\nu^3/\lambda^2 D , \quad (17b)$$

$$c=\nu^5/\lambda^4 D^2 . \quad (17c)$$

The generalized scaling relation Eq. (4) becomes (absorbing extra factors of 2 into the definition of the scaling function g)

$$w(L,t)=(\nu/|\lambda|) g(\lambda^2 D L/\nu^3, \lambda^4 D^2 t/\nu^5) . \quad (18)$$

We note that (18) allows us to predict scaling behavior outside the asymptotic region for the KPZ equation in $d=2$. In particular Eq. (18) predicts that the time t_c and length L_c for crossover from Edwards-Wilkinson behavior to KPZ behavior should scale as

$$L_c=(\nu^3/\lambda^2 D) L_0; \quad t_c=(\nu^5/\lambda^4 D^2)\tau_0 , \quad (19)$$

where L_0 and τ_0 are the corresponding quantities in the rescaled Eq. (2). Consideration of this equation may explain why some microscopic models cross over to KPZ behavior relatively quickly while others do not. From direct numerical simulations of the KPZ equation in $d=2$ we have quantitatively verified this dependence (see Sec. III). Of course, in any discrete model one expects that there will be additional irrelevant terms which may render this early-time behavior difficult to observe.

We now consider the *asymptotic* scaling relations in $d=2$. Inserting the known values for the exponents in $d=2$ ($\alpha=\frac{1}{2}$, $\beta=\frac{1}{3}$, and $z=\frac{3}{2}$) into the asymptotic scaling form Eq. (10) we obtain

$$w(L,t)=\sqrt{D/\nu} L^{1/2} f(|\lambda| \sqrt{D/\nu} t/L^{3/2}) , \quad (20)$$

where $f(x)$ is a universal scaling function characteristic of the KPZ equation in $d=2$ satisfying $f(x)=u_t x^{1/3}$ for $x \ll 1$ and $f(\infty)=u_L$. Equation (20) implies, in the limits $L \to \infty$ and $t \to \infty$, the relations

$$w(\infty,t)=u_t[|\lambda|(D/\nu)^2 t]^{1/3}=C_t t^{1/3} , \quad (21a)$$

$$w(L,\infty)=u_L \sqrt{D/\nu} L^{1/2}=C_L L^{1/2} , \quad (21b)$$

where u_L and u_t are universal (model-independent) constants characteristic of the KPZ equation fixed point in $d=2$, and $C_L=u_L\sqrt{D/\nu}$, while $C_t=u_t[|\lambda|(D/\nu)^2]^{1/3}$. Similarly, the modified scaling form Eq. (11) becomes

$$w(L,t)=C_L L^{1/2} F(|\lambda| C_L t/L^{3/2}) , \quad (22a)$$

where $F(x)=(1/u_L) f(x/u_L)$. Equation (22a) implies

$$w(\infty,t)=(u_t/u_L^{4/3})(|\lambda| C_L^4)^{1/3} t^{1/3}=C_t t^{1/3} \quad (22b)$$

so that we also obtain the universal amplitude ratio R in $d=2$,

$$R=C_t/(|\lambda| C_L^4)^{1/3}=u_t/u_L^{4/3} . \quad (23)$$

Similarly, Eq. (15) for the correlation function $G(x,t)$ at saturation becomes in $d=2$,

$$G(x,t)=A_x x F_G(|\lambda| \sqrt{A_x} t/x^{3/2}) , \quad (24)$$

where $F_G(0)=1$ and $F_G(u)=(g_t/g_x^{5/3}) u^{2/3}$ for $u \gg 1$. Analogous to Eq. (21), one may write for the correlation function amplitudes,

$$A_t=G(0,t)/t^{2/3}=g_t[|\lambda|(D/\nu)^2]^{2/3} , \quad (25a)$$

$$A_x=G(x,0)/x=g_x D/\nu , \quad (25b)$$

which implies the universal correlation function amplitude ratio,

$$R_G=A_t/(|\lambda| A_x^2)^{2/3}=g_t/g_x^{5/3} . \quad (26)$$

We note that the appearance of the parameter λ and the ratio D/ν in Eqs. (20)–(26) is appropriate, since from the renormalization-group equations in $d=2$ [3,4] one expects that the coarse-grained effective values of D and ν should scale with coarse-graining length as,

$D_{\rm eff}(bL)=b^{1/2}D_{\rm eff}(L)$ and $\nu_{\rm eff}(bL)=b^{1/2}\nu_{\rm eff}(L)$, while the parameter λ and the ratio D/ν remain invariant [18,19]. In addition, an analysis of the crossover exponent from $\lambda=0$ to finite λ from the renormalization-group equations leads to results for the dependence on λ that are consistent with Eqs. (20)–(26).

It is interesting to note that Eqs. (21b) and (25b) for the steady-state amplitudes C_L and A_x in $d=2$ are independent of λ and in fact have the same form as the corresponding equations for the linear ($\lambda=0$) case. This is not surprising, since the exponent $\alpha=\frac{1}{2}$ is the same for both cases. This suggests that the steady-state amplitudes are the same as for the linear case, and the universal coefficients u_L and g_x may be determined from the linear equation. This will be confirmed by our mode-coupling analysis. We note that a similar result has previously been obtained for the case of Burgers' equation in $d=2$ by Huse, Henley, and Fisher [20]. Thus, the interesting universal quantities are the early-time coefficients u_t and g_t and the amplitude ratios R and R_G. In addition, we point out that the universal quantities u_L and g_x may depend on boundary conditions, since the solution of the rescaled equation obviously depends on boundary conditions. The universal growth coefficients u_t and g_t should not depend on boundary conditions, however, since they are taken in the limit $t/L^z\to 0$.

Besides the amplitude ratios R and R_G, other universal ratios may also exist for the KPZ equation in $d=2$. For example, Krug and Meakin [21] have shown that the finite-size corrections to the saturation velocity have the form $V(L)=V(\infty)+C_V(\lambda)/L$ in $d=2$. Using the scale transformation (17), we obtain $C_V(\lambda)=u_V(\lambda D/\nu)$, where u_V is another universal constant and we have obtained the dependence of C_V on D and ν as well as on λ. This implies the existence of a universal amplitude ratio $R_V=C_V/[\lambda(C_L)^2]=u_V/u_L^2$. For the single-step model with random-site updating, it is known [21–24] that $C_V=-\frac{1}{2}$, $\lambda=-1$, and $C_L=1/\sqrt{12}$, which implies that $R_V=6.0$ and $u_V=\frac{1}{2}$. In Sec. IV we present the results of simulations of three different surface-growth models in $d=2$, which were conducted in order to test Eqs. (20)–(26) as well as to determine the universal amplitude ratios R, R_G, and R_V as well as the universal scaling function $F(x)$.

C. KPZ equation in $d=3$

In $d=d_c=3$, the transformation (9) diverges, and so a linear transformation that scales away all three parameters cannot be performed. Instead, we consider a transformation of the form

$$\nu\to\nu'=1=\nu c/b^2 , \tag{27a}$$

$$\lambda/2\to\lambda'/2=\epsilon=\lambda ac/2b^2 , \tag{27b}$$

$$2D\to 2D'=1=2Dc/a^2b^2 , \tag{27c}$$

where the parameter $\epsilon=\lambda^2D/\nu^3$ is dimensionless in $d=3$. This is similar to the transformation we used in a previous numerical study of the KPZ equation in $d=3$ [25]. Solving for a and b we find

$$a=\sqrt{2D/\nu},\quad b=\sqrt{\nu c} , \tag{28}$$

where the only condition on c is that it have the dimension of time so that $\mathbf{x}',h',t'$ are dimensionless. Substituting (23) into the generalized scaling relation (4), we obtain the generalized scaling form,

$$w(L,t)=\sqrt{D/\nu}\,f_\epsilon(L/\sqrt{\nu c},t/c) , \tag{29}$$

where the scaling function f now depends on the parameter ϵ. The ϵ dependence of f is an indication that a linear scale transformation (which would lead to a power-law dependence of ϵ in the scaling function) cannot be used to remove the parameter dependence in $d=3$. Setting c equal to one time unit, Eq. (29) may be rewritten,

$$w(L,t)=\sqrt{D/\nu}\,f_\epsilon(L/\sqrt{\nu},t) . \tag{30}$$

Equation (30) may be compared with the crossover scaling form proposed on the basis of renormalization-group analysis by Tang, Nattermann, and Forrest [13]. In the limit $L\to\infty$, they obtained

$$w^2(\infty,t)=\frac{D}{\nu}\left[\frac{8}{\epsilon}\right][G(\xi_0 t^{1/2}/e^{8\pi/\epsilon})+\ln(8\pi/\epsilon)] . \tag{31}$$

As in Eq. (30), we note the presence of a factor of D/ν. We also note that the time is not simply rescaled by a power of ϵ, but rather there is an exponential dependence. This is due to the fact that the nonlinear term (λ) is marginal (to first order) [3,13] at the critical dimension $d=3$.

D. Nonlinear molecular-beam-epitaxy (MBE) model

We now discuss the application of similar scaling ideas to the recently proposed nonlinear MBE model of Lai and Das Sarma [15]. For this model, the continuum interface equation is

$$\frac{\partial h}{\partial t}=-\nu_1\nabla^4 h+\lambda_1\nabla^2(|\nabla h|^2)+\eta \tag{32}$$

with

$$\langle\eta(\mathbf{x}_1',t_1')\eta(\mathbf{x}_2',t_2')\rangle=2D_1\delta^{(d-1)}(\mathbf{x}_1'-\mathbf{x}_2')\delta(t_1'-t_2') .$$

The scaling exponents are known to be $\alpha=(5-d)/3$, $\beta=(5-d)/(7+d)$, $z=(7+d)/3$ for $d<d_c=5$. Applying the scaling transformation Eq. (3), but requiring $\nu_1\to\nu_1'=1$, $\lambda_1\to\lambda_1'=1$, $2D_1\to 2D_1'=1$, we obtain

$$a=\nu_1/\lambda_1 , \tag{33a}$$

$$b=(\nu_1^3/2\lambda_1^2D_1)^{1/(5-d)} , \tag{33b}$$

$$c=(\nu_1^{7+d}/16\lambda_1^8D_1^4)^{1/(5-d)} , \tag{33c}$$

which is valid for $d<5$. Substituting into the general scaling form (5) we obtain the scaling form,

$$w(L,t)=(D_1/\lambda_1)^{1/3}L^{(5-d)/3}f(\lambda_1^{2/3}D_1^{1/3}t/L^{(7+d)/3}) \tag{34}$$

with $f(\infty)=u_L$ and $f(u)=u_t t^{(5-d)/(7+d)}$ for $u\ll 1$. This may be rewritten in the form

$$w(L,t)=C_L L^{(5-d)/3} F(\lambda_1 C_L t/L^{(7+d)/3}) , \quad (35)$$

where $C_L=u_L(D_1/\lambda_1)^{1/3}$ and $F(x)=1/u_L f(x/u_L)$. Equation (35) implies the existence of a universal amplitude ratio $R'=C_t/(C_L^{12}\lambda_1^{5-d})^{1/(7+d)}$ for this model where $C_t=u_t(D_1^4/\lambda_1^{d-1})^{1/(7+d)}$. As before, similar expressions may be written for the asymptotic correlation function $G(\mathbf{x},t)$. It is interesting to note that the parameter ν_1, although crucial for the observed scaling behavior, does not enter into the asymptotic scaling equations (34) and (35).

E. Conserved-noise growth model

Finally, we consider the conserved-noise growth model of Sun, Guo, and Grant [14]. The equation of evolution for this model is the same as Eq. (32), but with conserved noise of the form

$$\langle \eta(\mathbf{x}_1',t_1')\eta(\mathbf{x}_2',t_2')\rangle = -2D_1\nabla^2\delta^{(d-1)}(\mathbf{x}_1'-\mathbf{x}_2')\delta(t_1'-t_2') . \quad (36)$$

For this model, the scaling exponents are known to be $\alpha=(3-d)/3$, $\beta=(3-d)/(9+d)$, $z=(9+d)/3$ for $d<d_c=3$. Above $d_c=3$, the nonlinearity becomes irrelevant ($z=4$) and the exponents are the same as for the linear $\lambda_1=0$ version of the equation. From the same scaling analysis as above, we obtain $a=2\nu_1/\lambda_1$, $b=(2\nu_1^3/\lambda_1^2 D_1)^{1/(3-d)}$, and $c=b^4/\nu_1$, which in $d=2$ gives $a=2\nu_1/\lambda_1$, $b=2\nu_1^3/\lambda_1^2 D_1$, and $c=16\nu_1^{11}/\lambda_1^8 D_1^4$. For $d=2$ this implies,

$$w(L,t)=(D_1/\lambda_1)^{1/3}L^{1/3}f(\lambda_1^{2/3}D_1^{1/3}t/L^{11/3}) \quad (37)$$

or

$$w(L,t)=C_L L^{1/3}F(\lambda_1 C_L t/L^{11/3}) , \quad (38)$$

where $C_L=f(\infty)(D_1/\lambda_1)^{1/3}$. In addition, we obtain the universal amplitude ratio $R'=C_t/(C_L^{12}\lambda_1)^{1/11}$ in $d=2$.

III. MODE-COUPLING APPROXIMATION

As already noted, the scaling approach we have discussed so far is expected to be valid for $d\le d_c$ for each model. However, scaling arguments do not allow us to determine the scaling function or the values of the universal amplitude ratios. As a result, we now discuss the application of the mode-coupling approximation to the KPZ equation in $d=2$. We shall demonstrate that the mode-coupling approach not only reproduces the scaling forms already obtained, but also allows us to calculate the universal coefficient u_t and the amplitude ratio R as well as the scaling function $F(u)$. Similar results are also obtained for the correlation function $G(x,t)$.

The idea behind the mode-coupling approximation [26,27] is to assume that the nonlinear ($\lambda\neq 0$) KPZ equation (2) may be approximately solved by replacing the linear ($\lambda=0$) solution, which involves the coefficients D and ν, with $\mathbf{k}$-dependent coefficients $D(k)$ and $\nu(k)$, which are renormalized due to the nonlinearity. A similar approach has been used in a discussion of crossover behavior in the KPZ equation in $d=3$ by Tang, Nattermann, and Forrest [13]. Starting from a flat surface at $t=0$, the solution of the linear ($\lambda=0$) version of Eq. (2) may be written (see Appendix A) as

$$w^2(L,t)=\frac{1}{2\pi}\int_{-\infty}^{\infty}\frac{1}{k^2}\frac{D}{\nu}(1-e^{-2\nu k^2 t})dk . \quad (39)$$

For a system of finite-size L with a lower-length cutoff a, this may be rewritten as

$$w^2(L,t)=\frac{1}{\pi}\int_{\Lambda_L}^{\Lambda_a}\frac{1}{k^2}\frac{D}{\nu}(1-e^{-2\nu k^2 t})dk , \quad (40)$$

where $\Lambda_L\sim 1/L$ and $\Lambda_a\sim 1/a$ refer to upper and lower cutoffs, respectively. In the limit t, $L\to\infty$, and $t/L^2\to 0$, Eq. (40) implies

$$w^2(\infty,t)=\frac{2D}{\sqrt{2\pi\nu}}t^{1/2} , \quad (41)$$

which is independent of the cutoffs. From numerical integration of the KPZ equation with $\lambda=0$ for several values of D and ν, we have obtained very good agreement with Eq. (41).

For a discrete model of size L with periodic boundary conditions, Eq. (40) for the linear case should properly be written in the discretized form [22,28]

$$w^2(L,t)=\frac{2}{L}\sum_{m=1}^{L/2}\frac{1}{k_m^2}\frac{D}{\nu}(1-e^{-2\nu k_m^2 t}) , \quad (42a)$$

where $k_m=2\pi m/L$. In the limit $t\to\infty$, this becomes, for large L,

$$w^2(L,\infty)=\frac{D}{12\nu}L , \quad (42b)$$

which implies $u_L=\sqrt{1/12}$. From numerical integration of the Edwards-Wilkinson equation with periodic boundary conditions for a range of values of D and ν (see Sec. IV), we have obtained good agreement with Eq. (42b).

To implement the mode-coupling approximation we now substitute the length-scale-dependent parameters $D(k)$ and $\nu(k)$ obtained from the renormalization-group flow equations into the appropriate linear equation [either Eq. (40) or Eq. (42a) depending on the boundary conditions] above. To first order the renormalization-group equations for the KPZ equation, after rescaling by a factor $b=e^l$ and integrating over short-wavelength fluctuations, are in d dimensions [3,4]

$$\frac{d\nu}{dl}=\left[z-2+\frac{K_d g(3-d)}{4(d-1)}\right]\nu , \quad (43a)$$

$$\frac{dD}{dl}=\left[z-d+1-2\alpha+\frac{K_d g}{4}\right]D , \quad (43b)$$

$$\frac{d\lambda}{dl}=(\alpha+z-2)\lambda , \quad (43c)$$

where $K_d^{-1}=2^{d-2}\pi^{(d-1)/2}\Gamma((d-1)/2)$ and the dimensionless coupling parameter $g=(a/\pi)^{3-d}\lambda^2 D/\nu^3$. In $d=2$ these equations become

$$\frac{d\nu}{dl}=\left[-\tfrac{1}{2}+\frac{K_2 g}{4}\right]\nu , \quad (44a)$$

$$\frac{dD}{dl}=\left[-\tfrac{1}{2}+\frac{K_2 g}{4}\right]D\ , \tag{44b}$$

$$\frac{d\lambda}{dl}=(\alpha+z-2)\lambda\ , \tag{44c}$$

where $\alpha=\frac{1}{2}$ and $z=\frac{3}{2}$. We note that in $d=2$, D and ν satisfy the same scaling form so that the ratio $D(b)/\nu(b)$ is independent of length scale. Also, λ is independent of b due to the well-known scaling relation $\alpha+z=2$ (which follows as a result of Galilean invariance of the KPZ equation) [7,18].

Equation (44) with $\alpha+z=2$ implies that the dimensionless coupling parameter $g=(a/\pi)\lambda^2 D/\nu^3$ satisfies the flow equation,

$$\frac{dg}{dl}=g-K_2 g^2/2+O(g^3)\ , \tag{45}$$

which has two fixed points, a trivial fixed point at $g=0$ and a strong-coupling (finite λ) fixed point at $g^*=2/K_2=2\pi$. Integrating we obtain

$$g(b)=\frac{g_B b}{1+(g_B/g^*)(b-1)}\ , \tag{46}$$

where $g_B=g(1)$ is the bare value of the dimensionless coupling constant. Substituting Eq. (46) for $g(b)$ into (44a) and (44b) and integrating we obtain

$$\nu(b)=\nu_B[(1-\alpha_B)+\alpha_B b]^{1/2}\ , \tag{47a}$$

$$D(b)=D_B[(1-\alpha_B)+\alpha_B b]^{1/2}\ , \tag{47b}$$

where

$$\alpha_B=K_2 g_B/2=\frac{a}{2\pi^2}\frac{\lambda^2 D_B}{\nu_B^3}\ .$$

As already mentioned, $D(b)$ and $\nu(b)$ scale the same way so that the ratio $D(b)/\nu(b)=D_B/\nu_B$ is independent of the rescaling factor b.

In order to implement the mode-coupling approximation for $\lambda\neq 0$ for periodic boundary conditions we now replace D and ν in the Edwards-Wilkinson solution Eq. (42a) with $D(k)$ and $\nu(k)$ using Eq. (47), with $b\sim k^{-1}$. Because of the uncertainty in the correct scaling factor between b and $1/k$, we do not expect our mode-coupling results to be exact. However, we expect the mode-coupling approximation to give the correct scaling form as well as a reasonable estimate of the universal amplitude ratios. In addition, as suggested earlier by our scaling results, our mode-coupling calculation confirms that the universal steady-state coefficients are the same for the nonlinear case as for the linear case. We expect this last result to be exact, since it depends only on the fact that $D(k)$ and $\nu(k)$ scale the same way, a result expected to hold to all orders of perturbation theory [3,4]. In what follows below, we take $b=S_c/ka$, where S_c is an unknown scaling factor of $O(1)$ between b and $1/k$. Typically, we will take $S_c=1$ at the end of our calculations, however in order to show the dependence of our final results on this factor, we will keep the factor S_c in our expressions.

Substituting $D(k)$ and $\nu(k)$ from Eq. (47) (taking $b=S_c/ka$), Eq. (42a) then becomes (setting a equal to 1)

$$w^2(L,t)=\frac{2D}{L\nu}\sum_{m=1}^{L/2}\frac{1}{k_m^2}(1-e^{-[A+B^2/k_m]^{1/2}k_m^2 t})\ , \tag{48}$$

where $A=(2\nu_B)^2(1-\alpha_B)$ and

$$B=2\nu_B(\alpha_B S_c)^{1/2}=\frac{\sqrt{2S_c}}{\pi}|\lambda|\sqrt{D/\nu}\ ,$$

and we have removed the bare subscript since (D/ν) is independent of the rescaling factor b. In the long-time limit, the exponential goes to zero, and we recover the linear result $w^2(L,\infty)=(D/12\nu)L$, with $u_L=1/\sqrt{12}$.

We now consider the asymptotic limit of Eq. (48) for large L,t in order to obtain the mode-coupling prediction for the universal scaling function. In the limit $t\to\infty$, Eq. (48) may be rewritten,

$$w^2(L,t)=\frac{2D}{L\nu}\sum_{m=1}^{L/2}\frac{1}{k_m^2}(1-e^{-Bk_m^{3/2}t}) \tag{49}$$

since for $k_m\sim 1/L\to 0$, the second term in the brackets (B^2/k_m) in Eq. (48) will dominate over the A term, while for k_m finite, the exponential factor goes to zero and is irrelevant. It is interesting to note that if $g_B=g^*$ (i.e., $A=0$) then Eq. (49) holds even for small t, so that the asymptotic limit is reached immediately.

Substituting

$$k_m=2\pi m/L$$

and

$$B=(\sqrt{2S_c}/\pi)|\lambda|\sqrt{D/\nu}\ ,$$

Eq. (49) may be rewritten in the scaling form (taking the limit $L\to\infty$),

$$f^2(u)=\frac{w^2(L,t)}{\left[\frac{D}{\nu}\right]L}=\frac{1}{2\pi^2}\sum_{m=1}^{\infty}\frac{1}{m^2}(1-e^{-4\sqrt{\pi S_c}m^{3/2}u}), \tag{50}$$

where $u=|\lambda|\sqrt{D/\nu}\,t/L^{3/2}$, $f(u)=u_t u^{1/3}$ for $u\ll 1$, and $f(\infty)=u_L=1/\sqrt{12}$. Thus, from the mode-coupling approximation we have derived the scaling form predicted in Eq. (20) for the case of periodic boundary conditions. The detailed evaluation of $f(u)$ requires numerical summation of Eq. (50).

From Eq. (50), we may calculate the universal growth coefficient u_t by noting that in the limit $u\to 0$, the only nonzero contributions to the sum are for large m, so that in this limit the summation may be converted to the integral,

$$f^2(u)\to\frac{(4\sqrt{\pi S_c}u)^{2/3}}{3\pi^2}\int_0^{\infty}\frac{1}{y^{5/3}}(1-e^{-y})dy$$
$$=\Gamma(\tfrac{1}{3})(2S_c)^{1/3}\pi^{-5/3}u^{2/3}\ , \tag{51}$$

where $y=4\sqrt{\pi S_c}m^{3/2}u$. From this, we obtain the universal growth coefficient $u_t=[\Gamma(\frac{1}{3})(2S_c)^{1/3}\pi^{-5/3}]^{1/2}$. Taking S_c equal to 1, yields $u_t=0.71$ and the universal amplitude ratio $R=u_t/u_L^{4/3}\simeq 3.7$.

In order to compare with simulations, we may also calculate the scaling function in the form

$$F(x)=w(L,t)/C_L L^{1/2}=\frac{1}{u_L}f(x/u_L)\ ,$$

where $x=|\lambda|C_L t/L^{3/2}$. In this form Eq. (50) becomes

$$F^2(x)=\frac{6}{\pi^2}\sum_{m=1}^{\infty}\frac{1}{m^2}(1-e^{-8\sqrt{3\pi S_c}m^{3/2}x})\ , \tag{52}$$

where $F(x)=(u_t/u_L^{4/3})x^{1/3}$ for $x\ll 1$, $F(\infty)=1$. In the next section we will present the results of a numerical evaluation of (52) as well as comparisons with simulations of discrete models.

While convenient for computer simulations, periodic boundary conditions are not particularly relevant for experiments. More appropriate perhaps, are free boundary conditions (for which the corresponding universal coefficient may be denoted u_L^f), in which the surface width $w_f(L,t)$ is measured over a region L embedded in a much larger system of size N. In particular, this type of measurement has been used in the analysis of recent experiments in $d=2$ on flow in porous media by Rubio *et al.* [29] and Horváth *et al.* [30], as well as in simulations by Martys, Cieplak, and Robbins [31]. From the solution of the linear equation, we obtain for this case (see the Appendix) $u_L^f=1/\sqrt{6}=\sqrt{2}u_L$. This result is also in agreement with an analytic calculation (Appendix) we have done for the single-step model as well as simulation results we have obtained for the restricted solid-on-solid (RSOS) model. For completeness, we now present our results for the scaling function $\hat{f}(u)$ for this case. We denote the corresponding universal amplitude ratio as $R^f=C_t/[|\lambda|(C_L^f)^4]^{1/3}=u_t/(u_L^f)^{4/3}=R/2^{2/3}$.

From Eq. (A7), we obtain for the linear equation with free boundary conditions,

$$w_f^2(L,t)=\frac{2D}{\pi\nu L^2}\int_{\Lambda_N}^{\Lambda_a}\frac{1}{k^4}\left[\frac{(kL)^2}{2}-1+\cos(kL)\right]\times(1-e^{-2\nu k^2 t})dk\ , \tag{53}$$

where $\Lambda_N\sim 1/N$ and $\Lambda_a\sim 1/a$. Substituting, $D(k)$ and $\nu(k)$ in (53) as before, noting again that small k dominates the exponential in the asymptotic limit, and making the substitution $y=kL$, we obtain

$$w_f^2(L,t)=\frac{2DL}{\pi\nu}\int_0^{\infty}\frac{1}{y^4}\left[\frac{y^2}{2}-1+\cos(y)\right]\times(1-e^{-By^{3/2}t/L^{3/2}})dy\ , \tag{54}$$

where B is the same as before, and the limits on the integral have been taken in the limit $N,L\to\infty$, $L/N\to 0$. This implies the scaling form for the free boundary condition case,

$$\hat{f}^2(u)=\frac{w_f^2(L,t)}{\left[\frac{D}{\nu}\right]L}=\frac{2}{\pi}\int_0^{\infty}\frac{1}{y^4}[y^2/2-1+\cos(y)]\times(1-e^{-\sqrt{2S_c}y^{3/2}u/\pi})dy\ , \tag{55}$$

where $u=|\lambda|\sqrt{D/\nu}\,t/L^{3/2}$, $\hat{f}(u)=u_t u^{1/3}$ for $u\ll 1$ (with u_t the same as for the case of periodic boundary conditions), and $\hat{f}(\infty)=u_L^f=1/\sqrt{6}$. Since $R^f=R/2^{2/3}$, we obtain $R^f\simeq 2.3$.

The mode-coupling approximation can also be used to calculate scaling expressions for the height-height correlation function $G(x,t)=\langle[\tilde{h}(x'+x,t'+t)-\tilde{h}(x',t')]^2\rangle$, where $\tilde{h}(x,t)=h(x,t)-\langle h(x,t)\rangle_x$ in the saturation limit $t'\gg L^z$. In this limit, the solution of the linear ($\lambda=0$) equation for the correlation function $G(x,t)$ becomes (see the Appendix)

$$G(x,t)=\frac{2}{\pi}\int_{\Lambda_L}^{\Lambda_a}\frac{1}{k^2}\frac{D}{\nu}[1-\cos(kx)e^{-\nu k^2 t}]dk\ . \tag{56}$$

In the asymptotic limits in which we are interested ($x,t,L\to\infty, x/L\to 0, t/L^z\to 0$) the details of the cutoffs on the integral will turn out to be irrelevant. Substituting $D(k),\nu(k)$ as before and noting that small k dominates the exponential in the asymptotic limit $t\to\infty$, we obtain,

$$G(x,t)=\frac{2D}{\pi\nu}\int_{\Lambda_L}^{\Lambda_a}\frac{1}{k^2}[1-\cos(kx)e^{-B'k^{3/2}t}]dk\ , \tag{57}$$

where $B'=(1/\pi)\sqrt{S_c/2}|\lambda|\sqrt{D/\nu}=B/2$.

For the case of the equal-time ($t=0$) correlation function, Eq. (57) implies that for $x,L\to\infty$, $x/L\to 0$, we recover the linear result

$$G(x,0)=\frac{2D}{\pi\nu}x\int_0^{\infty}\frac{1}{y^2}[1-\cos(y)]dy=\frac{D}{\nu}x=A_x x \tag{58}$$

so that $g_x=A_x/(D/\nu)=1$.

Similarly for the case $x=0$, Eq. (57) becomes, making the substitution $y=B'k^{3/2}t$, and in the limit $t,L\to\infty$ with $t\ll L^{3/2}$,

$$G(0,t)=\frac{4DB'^{2/3}t^{2/3}}{3\pi\nu}\int_0^{\infty}\frac{1}{y^{5/3}}(1-e^{-y})dy=g_t\left[\frac{|\lambda|D^2 t}{\nu^2}\right]^{2/3}=A_t t^{2/3}\ , \tag{59}$$

where $g_t=2^{2/3}\Gamma(\frac{1}{3})S_c^{1/3}/\pi^{5/3}$. We note that (58) and (59) imply that if $G(x,0)=A_x x$, then $G(0,t)=g_t(|\lambda|A_x^2 t)^{2/3}$, so that $R_G=g_t=A_t/(|\lambda|A_x^2)^{2/3}$. Taking $S_c=1$ yields $R_G\simeq 0.63$.

Finally, we may use Eq. (57) to compute a general scaling function for $G(x,t)$ of the form

$$G(x,t)=(D/\nu)x\,f_G(|\lambda|\sqrt{D/\nu}\,t/x^{3/2})\ , \tag{60}$$

which is the same as Eq. (24), with $A_x=D/\nu$. Making the substitution $y=kx$, Eq. (57) becomes in the limit $x,t\to\infty$, $x\ll L$,

$$G(x,t)=\frac{2Dx}{\nu\pi}\int_0^{\infty}\frac{1}{y^2}[1-\cos(y)e^{-B'y^{3/2}t/x^{3/2}}]dy\ . \tag{61}$$

This implies the existence of a scaling function of the form

$$f_G(u)=\frac{G(x,t)}{\left[\frac{D}{\nu}\right]x}$$
$$=\frac{2}{\pi}\int_0^\infty \frac{1}{y^2}[1-\cos(y)e^{-y^{3/2}\sqrt{S_c/2}\,u/\pi}]dy\ , \quad (62)$$

where $u=|\lambda|\sqrt{D/\nu}\,t/x^{3/2}$, $f_G(0)=1$, and $f_G(u)\to g_t u^{2/3}$ for $u\gg 1$. In the next section we present the results of extensive simulations of several different surface-growth models in $d=2$ which we conducted in order to test our scaling predictions, as well as the numerical values obtained from the mode-coupling approximation.

IV. NUMERICAL SIMULATIONS

A. Discrete models

In order to test our scaling analysis and mode-coupling-approximation predictions, we have simulated three different growth models which are believed to be in the KPZ universality class in $d=2$. The first two models—a RSOS growth model [9] and the single-step model [7,22]—were studied as a function of driving force f, while the ballistic deposition model [7] was studied in the irreversible limit. In the RSOS growth model each site to be updated attempts either to grow ($h\to h+1$) with probability $p_+=(1+f)/2$ or to shrink ($h\to h-1$) with probability $p_-=(1-f)/2$, subject to the RSOS restriction $|h(i)-h(i\pm1|\le 1$. Similarly, in the reversible single-step model the growth rule is $h(i)\to h(i)\pm 2$, subject to the same nearest-neighbor height restriction as in the RSOS model, with the initial state given by $h(i)=0$ for i odd, and $h(i)=1$ for i even. The value $f=0$ corresponds to completely reversible ($\lambda=0$) growth, while $f=1$ corresponds to completely irreversible growth. Finally, for the ballistic deposition model the growth rule is $h(i)\to Max[h(i+\delta),h(i)+1]$, where δ refers to nearest neighbors. We used a parallel updating scheme in which either an odd or an even sublattice was selected, while each growth-shrink step was attempted on each site of the selected sublattice with probability $\frac{1}{2}$ and periodic boundary conditions were used. For the RSOS model the sublattices were chosen randomly, while for the other two models odd and even sublattices alternated. Our unit of time is one full sweep of the lattice, and our length unit is simply the lattice spacing.

In our simulations the driving force f was varied from 0.5 to 1.0. For each value of f, the saturation width coefficient $C_L=w(L,\infty)/L^{1/2}$ was measured. The nonlinearity parameter λ was also measured by determining the change in the average saturation velocity V_L as a function of overall tilt $|\nabla h|$ for systems of size $L=512$. The tilt in the interface was enforced by using screw boundary conditions as in Ref. [32] and averages were taken over times of the order of 10^7 Monte Carlo steps (MCS). Figure 1 shows typical plots of the saturation velocity as a function of tilt for the RSOS model for $f=0.5$, 0.75, and 1.0. Similar plots for the single-step model are shown in Fig. 2. We found that λ was roughly

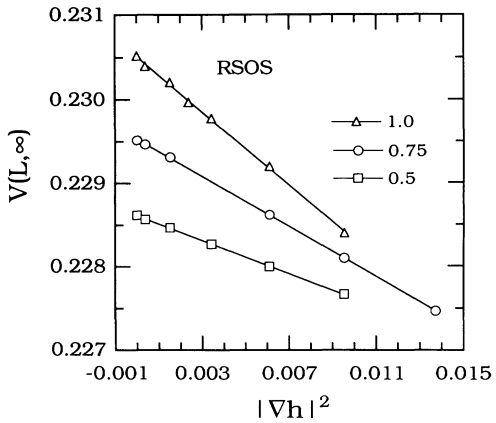

FIG. 1. Saturation velocity V_L vs $|\nabla h|^2$ for the RSOS model ($L=512$) for $f=1.0$ (triangles), $f=0.75$ (circles), $f=0.5$ (squares). Data for $f=0.75$ and $f=0.50$ have been shifted up by 0.0637 and 0.1206, respectively, for clarity. Solid lines are linear fits with slope $\lambda/2=-0.22$, -0.15, and -0.10.

(but not exactly) proportional to the driving force f and almost exactly proportional to the velocity as expected.

Figure 3 shows our results for the saturation width $w(L,\infty)$ as a function of system size L for the RSOS and single-step models for different values of the driving force f. The widths were obtained from averages over very long runs of the order of 10^7 MCS. Similar data were obtained for the ballistic deposition model. Surprisingly, we find little variation of the surface width with driving force f for a fixed system size for both the RSOS and single-step models. From the best fits to the data, we obtained for the RSOS model $C_L=0.230\pm0.003$, while for the single-step model and ballistic deposition model we obtained $C_L\simeq 0.28$ and $C_L\simeq 0.22$, respectively [33]. For the single-step model, it is not completely surprising that C_L is independent of driving force f, since it is known for the case of random updating [22,34] that $C_L=1/\sqrt{12}\simeq 0.29$ is independent of driving force. This is slightly larger than the measured value for C_L, which is

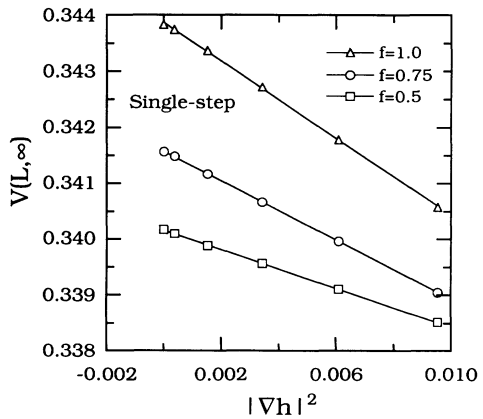

FIG. 2. Same as Fig. 1 but for single-step model. Data for $f=0.75$ and $f=0.50$ have been shifted up by 0.087 and 0.172, respectively, for clarity. Solid lines are linear fits with slope $\lambda/2=-0.340$, -0.265, and -0.172.

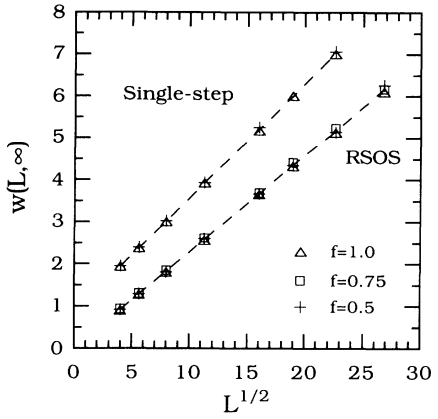

FIG. 3. Saturation width $w(L,\infty)$ vs $L^{1/2}$ ($L=16$–720) for the reversible single-step model and RSOS model with alternate sublattice updating, for different values of the parameter f. Dashed-line fits have slope $C_L=0.28$ for the single-step model and $C_L=0.23$ for the RSOS model.

most likely due to crossover effects.

The early-time behavior of the surface width $w(L,t)$ was also measured for each value of the driving force f and for each model. Simulations with very large system sizes ($L=262\,144$, averaged over 20 runs) were used in order to avoid saturation effects. Simulations were carried out for times of the order of 2×10^4 MCS, so that for all values of f the expected asymptotic $t^{1/3}$ behavior was observed at late times. Plots of the surface width $w(L,t)$ for the RSOS model for five values of f are shown in Fig. 4(a), while Fig. 4(b) shows the same data, with the time t scaled according to Eq. (22b) by the factor $(\lambda C_L^4)^{1/3}$, using the measured values of λ and C_L. Equation (23) implies that $C_t=R(\lambda C_L^4)^{1/3}$ so that at late times (when $t^{1/3}$ behavior is observed) the data in Fig. 4(b) should all be superimposed. We see that as predicted there is reasonably good data collapse even at early times. Figure 4(c) shows a log-log plot of the same data showing the approach to the $\frac{1}{3}$-exponent behavior. Similar data are shown in Fig. 5(a) for the single-step model, along with the scaled data in Fig. 5(b) which again show a reasonable data collapse. We note that if the scaled data for the RSOS model and single-step model are plotted in the same graph, they agree reasonably well even at early time.

For each value of f and for each model, the coefficient C_t was determined from fits of the form $w(L,t)=C_t t^{1/3}+b$ to the late-time data. Fits to this form as well as fits from log-log plots yielded the same value of C_t within a few percent. The amplitude ratio $R=C_t/(\lambda C_L^4)^{1/3}$ was then calculated from the measured values of C_t and C_L. Figure 6 shows a summary of our results for the amplitude ratio R plotted as a function of the scaling parameter $|\lambda|C_L^4$. As predicted by our scaling and mode-coupling analysis, R is essentially universal for all models and values of f. From the average of the data we obtain $R=3.45\pm0.05$. Figure 7 shows the same data for all three growth models in the form of a log-log plot of C_t versus $|\lambda|(C_L)^4$. In agreement with the scaling prediction (23) all the points lie on a universal line of slope equal to $\frac{1}{3}$. From the y intercept of the straight-line fit to this data we obtain $R\simeq3.42$. We note that these values of R are close to our mode-coupling-approximation prediction $R=3.7$.

In order to test the universality of the scaling function for the width in Eq. (22) we also determined $w(L,t)$ for a

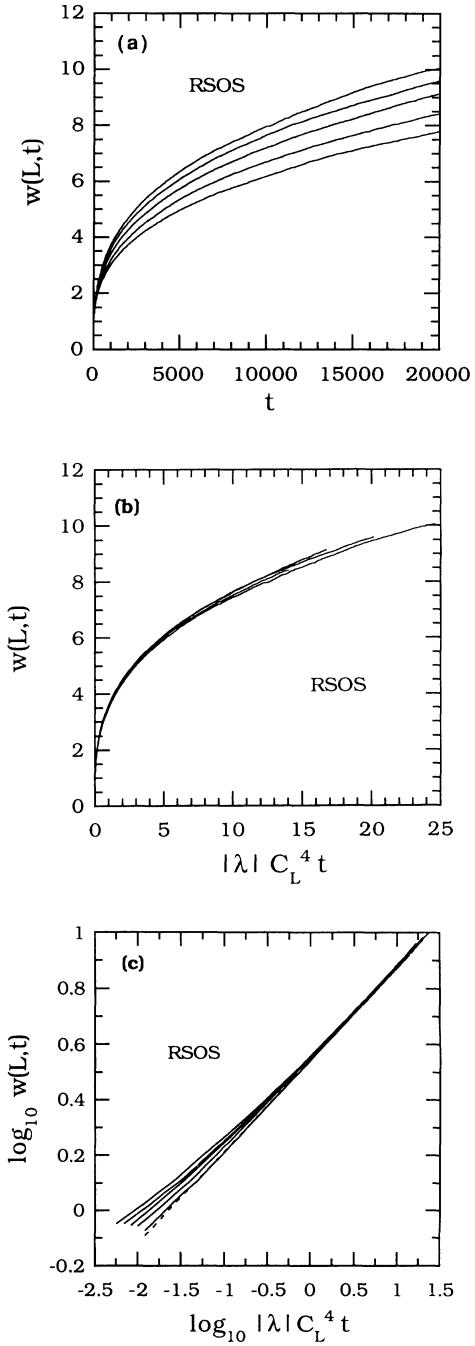

FIG. 4. (a) $w(L,t)(L=262\,144)$ vs t for (top to bottom) $f=1.0$, 0.866, 0.75, 0.612, and 0.5 for the reversible RSOS model. (b) Same as (a) but with time scaled by a factor of $|\lambda|C_L^4$. (c) Log-log plot of RSOS data scaled as in Eq. (22b). Dashed line has slope 0.33.

system of intermediate size ($L=2048$) from early-time to saturation for both the single-step model and the RSOS growth model with $f=1$. Averages were taken over 256 runs of 80 000 MCS. Figure 8(a) shows a scaling plot of our results. The asymptotic scaling functions for both models are essentially identical when scaled in the form of (22a) as predicted by our scaling analysis. Also shown is the mode-coupling prediction Eq. (52) for the scaling function with periodic boundary conditions, which has been numerically summed with $S_c=1$. Although we do not expect the mode-coupling approximation to be exact, we see that there is reasonable agreement. Thus, our simulation results for the surface width appear to confirm the validity of our scaling results in $d=2$. Figure 8(b) shows a log-log plot of the data in Fig. 8(a).

We have also analyzed the scaling properties of the correlation function $G(x,t)$ in order to determine the universal amplitude ratio R_G. Simulations were conducted on the single-step model, since this model appears to show asymptotic behavior even for small size. In order to compare with our previous simulations, we first calculated $G(0,t)$ for the irreversible ($f=1$) single-step model with alternate sublattice updating. We note that for the random-site updating version of this model, $A_x=1$, since at saturation the interface may be shown [34] to be a random walk of steps of height ± 1. We expect this to be true as well for our parallel-updating version since A_x is a steady-state quantity, and from measurement of $G(x,0)$ directly, we obtained $A_x \simeq 0.95$. Figure 9 shows our data for $G(0,t)$. The data fits the expected form $G(0,t)=A_t t^{2/3}$ with coefficient $A_t \simeq 0.55$. Using our measured value $\lambda \simeq -0.68$ and $A_x=1$ we obtain $R_G=A_t/(|\lambda| A_x^2)^{2/3} \simeq 0.71$. We note that our mode-coupling prediction $R_G \simeq 0.63$ is slightly below this value. Also shown in Fig. 9 is $G(0,t)$ for the single-step model with random-site updating for which $A_t \simeq 0.71$. For this model, it is known [21,23,24] that $\lambda=-1$ (as well as $A_x=1$) so that we again obtain $R_G=0.71$.

We also tested our scaling predictions for the saturation velocity amplitude ratio $R_V=C_V/(\lambda C_L^2)$, which is expected to have the value $R_V=6.0$ as was noted earlier from known properties of the random-site updating single-step model. From simulations of the irreversible

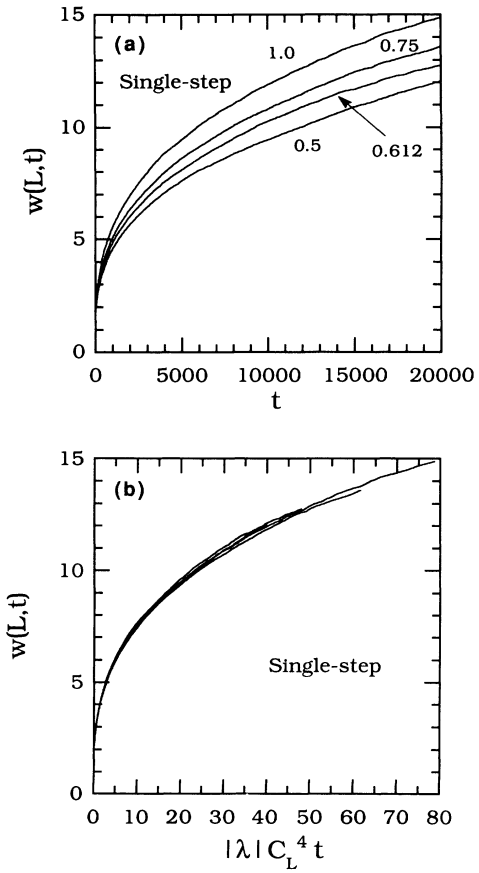

FIG. 5. (a) $w(L,t)(L=262\,144)$ vs t for (top to bottom) $f=1.0$, 0.75, 0.612, and 0.5 for the single-step model. (b) Same as (a) but with time scaled by a factor of $|\lambda| C_L^4$.

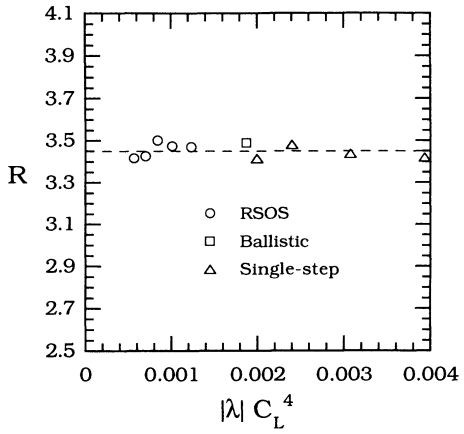

FIG. 6. Numerical estimates for amplitude ratio $R=C_t/(|\lambda| C_L^4)^{1/3}$ from data for RSOS, single-step, and ballistic deposition models for different values of the driving force f. Average value (dashed line) is 3.45 ± 0.05.

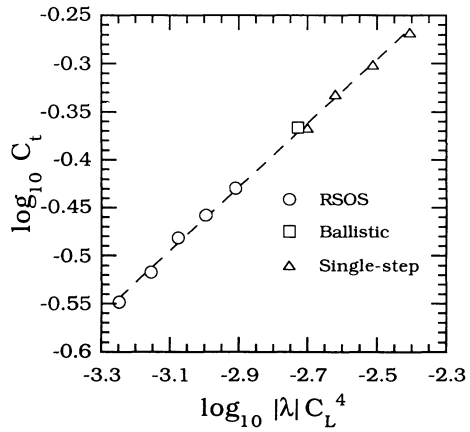

FIG. 7. Log-log plot of C_t vs $|\lambda| C_L^4$ for all three growth models. Circles are for RSOS model ($f=0.5$, 0.612, 0.75, 0.866, and 1.0), triangles are for single-step model ($f=0.5$, 0.612, 0.75, and 1.0), and square is for ballistic deposition model. Dashed-line fit has slope 0.331 ± 0.005.

RSOS growth model with alternate sublattice updating, we obtained $\lambda=-0.44$ and $C_L=0.23$, and $C_V\simeq-0.154$, which implies $R_V\simeq 6.6$. For our single-step model, using $\lambda=-0.68$, $C_L\simeq 0.276$, and $C_V=-0.335$ we obtain $R_V\simeq 6.4$. However, using the known asymptotic value of $C_L=1/\sqrt{12}$ for the single-step model (which should not depend on whether our updating is parallel or random), we obtained $R_V=5.95$, in much better agreement with the expected value $R_V=6.0$. Thus, we expect that the fact that our values are slightly higher than expected is mainly due to crossover effects. In Table I, we summarize our results for the amplitudes λ, C_t, C_L, A_x, and A_t, and amplitude ratios R and R_G for our discrete models.

As a test of a somewhat weaker form of universality, we have also studied the scaled-height-fluctuation distribution functions $P(X)$ at saturation in $d=2$, where $X=\delta h/w(L,\infty)$ is the local height fluctuation scaled by the rms total height fluctuation ($\delta h=h-\langle h\rangle$). Figure 10(a) shows the scaled-height-fluctuation distribution functions for two different growth models in $d=2$ at saturation. One model is the irreversible RSOS model ($f=1$) with random-site updating [9], while the other is a variation of the ballistic deposition model, in which the deposited particle heights are uniform random numbers between 0 and 1. The distributions are essentially identical for the two models. Figure 10(b) shows semilog plots of the same data, indicating that the distribution at saturation is Gaussian as expected [10,20] and can be fit to the form $P(X)=(1/\sqrt{2\pi\sigma^2})e^{-X^2/2\sigma^2}$. The slope of the fits, which is close to $\frac{1}{2}$, indicates that $\sigma=1$, since scaling

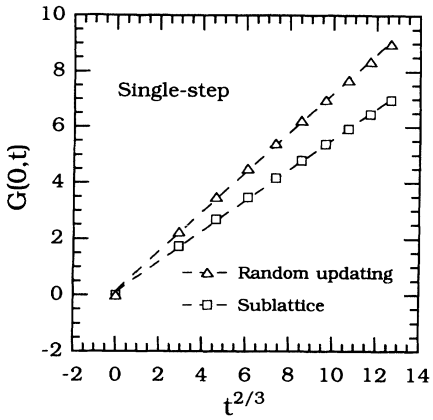

FIG. 9. $G(0,t)$ vs $t^{2/3}$ for single-step model ($f=1$) with random-site updating (triangles) and with alternate sublattice updating (squares). Dashed lines are linear fits to data with slopes $A_t=0.71$ and $A_t=0.55$.

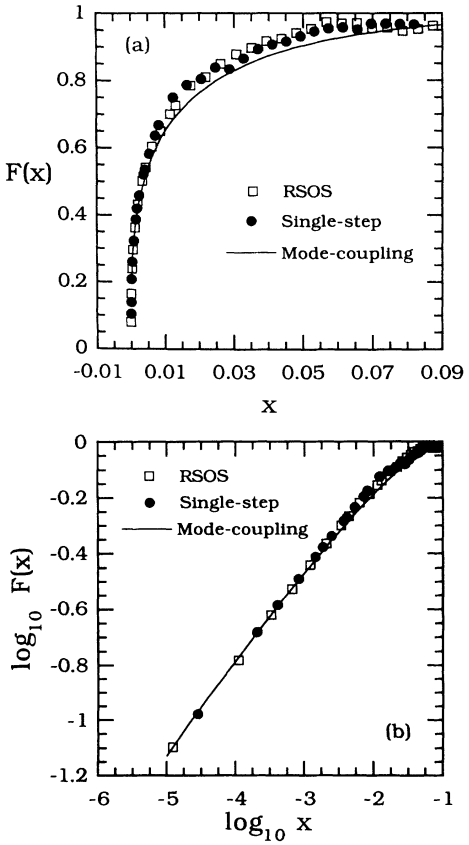

FIG. 8. (a) Scaling function $F(x)=w(L,t)/(L^{1/2}C_L)$, where $x=|\lambda|C_Lt/L^{3/2}$ [see Eq. (22)] from simulations of single-step model and RSOS model ($f=1$). Solid line is from numerical summation of Eq. (52), with $S_c=1$. (b) Log-log plot of (a) showing behavior for small x.

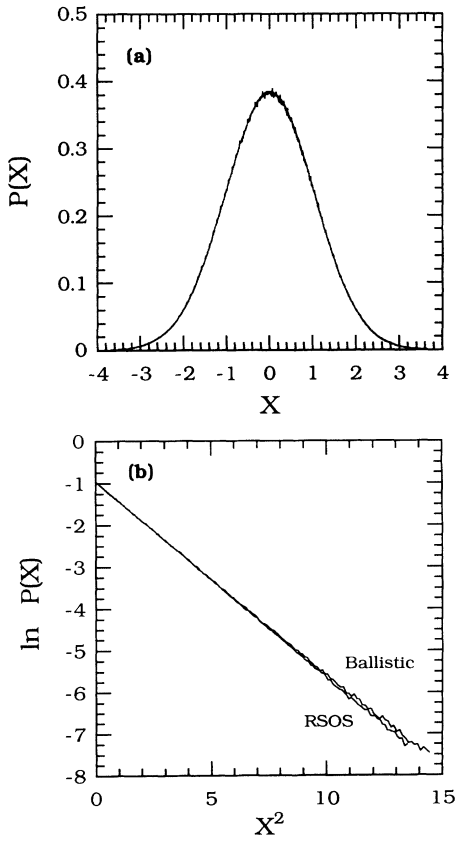

FIG. 10. (a) Distribution functions $P(X)$ for the scaled-height-fluctuation $X=\delta h/w(L,\infty)$ at saturation ($L=512$) for RSOS model and continuous ballistic deposition model with $f=1$. (b) Semilog plot of distribution functions $P(X)$ in (a). Linear fits have slope -0.46 (RSOS) and -0.47 (ballistic deposition).

TABLE I. Summary of results from discrete model simulations for amplitudes λ, C_t, C_L, A_x, and A_t, and amplitude ratios R and R_G.

Model	f	λ	C_t (A_t)	C_L, C_L^f, A_x	R (R_G)
RSOS	0.5	−0.20	0.283	0.23	3.43
	0.612	−0.25	0.304		3.42
	0.75	−0.30	0.330	0.23	3.50
	0.866	−0.36	0.348		3.48
	1.0	−0.44	0.372	0.23,0.34	3.47
Ballistic	1.0	0.83	0.43	0.218,0.313,0.588	3.49
Single-step	0.5	−0.344	0.43	0.276	3.41
	0.612	−0.414	0.466		3.48
	0.75	−0.53	0.50		3.44
	1.0	−0.68	0.54 (0.55)	0.276,0.145,0.95	3.42 (0.71)

the height fluctuations by the saturation width implies that $(\Delta X)^2=1$. We have previously observed similar behavior in a study [35] of the Zhang model [36] with power-law noise in which a cutoff in the range of the noise was introduced. As the system size was increased (for a fixed cutoff), the exponents crossed over from those appropriate to power-law noise to the ordinary KPZ values $\alpha=\frac{1}{2}$, $\beta=\frac{1}{3}$, while the height-fluctuation distribution crossed over from a power-law tail [37] to Gaussian distribution.

We note that a study of the scaled distribution functions (for the related directed polymer problem at $T=0$ and for the ballistic deposition model) has been recently carried out in the early-time regime by Kim, Moore, and Bray [38]. For both models, they found that the scaled distribution was universal and asymmetric. More recently this work has been extended for the directed polymer problem by Krug, Meakin, and Halpin-Healy [28]. An analytical determination of this distribution function in the early-time regime remains a challenging problem.

B. KPZ equation

We have also numerically integrated the KPZ equation in $d=2$ in order to determine the universal coefficients u_t and u_L and the universal amplitude ratio R directly. The KPZ equation was integrated on a lattice with grid spacing Δx and system size L (in units of Δx) using the discrete representation [25]

$$h(i,t+1)=h(i,t)+\Delta t(\nu/\Delta x^2)[h(i+1,t)-2h(i,t)+h(i-1,t)] +\Delta t(\lambda/8\Delta x^2)[h(i+1,t)-h(i-1,t)]^2+\sqrt{2D\Delta t/\Delta x}\,\xi(i,t)\ , \tag{63}$$

where $\xi(i,t)$ is Gaussian noise of unit strength independently generated at each site. Typically, we took $\Delta x=1$ or $\Delta x=\frac{1}{2}$ while Δt was taken to be 0.005 or 0.01, and periodic boundary conditions were used. Care was taken to keep Δt small enough so that we obtained reasonably good convergence, i.e., the results were independent of Δt. As a test of our integration scheme, we first studied the linear ($\lambda=0$) case for a variety of values of D and ν and obtained good agreement [39] with the exact result $w^2(L,\infty)=2Dt^{1/2}/\sqrt{2\pi\nu}$ [Eq. (41)].

As a further test of our integration scheme as well as of our scaling predictions (21b) and (25b), we also measured the steady-state quantities u_L and g_x directly. Figure 11 shows plots of the saturation width $w(L,\infty)$ as a function of system size L from integration of the KPZ equation with $D=\frac{1}{2}$, $\nu=1$ ($\Delta x=1, \Delta t=0.005$), and two different values of λ. We see that within fluctuations, the saturation width is essentially independent of λ as predicted. From the slope of the best fit to the data, we obtain $u_L=C_L/\sqrt{D/\nu}\simeq 0.29$, which is in reasonable agreement with the value $u_L=1/\sqrt{12}$ (0.288) predicted by Eq. (42b) for the case of periodic boundary conditions. The correlation function $G(x,0)$ (for a system of size $L=512$) was also measured (see Fig. 12) for two different values of λ and as expected, very little dependence on λ was found. The slope of the fit is about 0.45 in approximate agreement with the mode-coupling prediction $A_x=D/\nu=0.5$. The value obtained is slightly lower than predicted, most

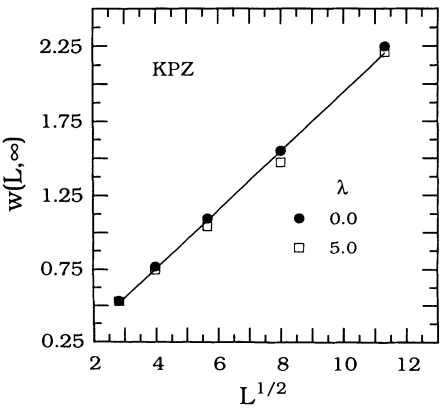

FIG. 11. $w(L,\infty)$ vs $L^{1/2}$ from numerical integration of the KPZ equation for $D=0.5$, $\nu=1.0$, with $\lambda=0$ and 5. Solid-line fit has slope $C_L=0.20\pm0.01$.

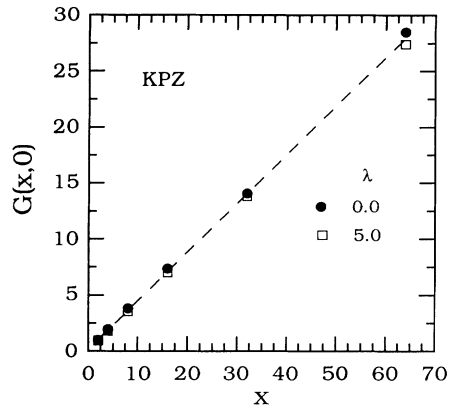

FIG. 12. Equal-time correlation function $G(x,0)$ from numerical integration of the KPZ equation on system of size $L=512$, $D=0.5$, $\nu=1.0$ for $\lambda=0$ and 5. Dashed-line fit has slope $A_t \simeq 0.45$.

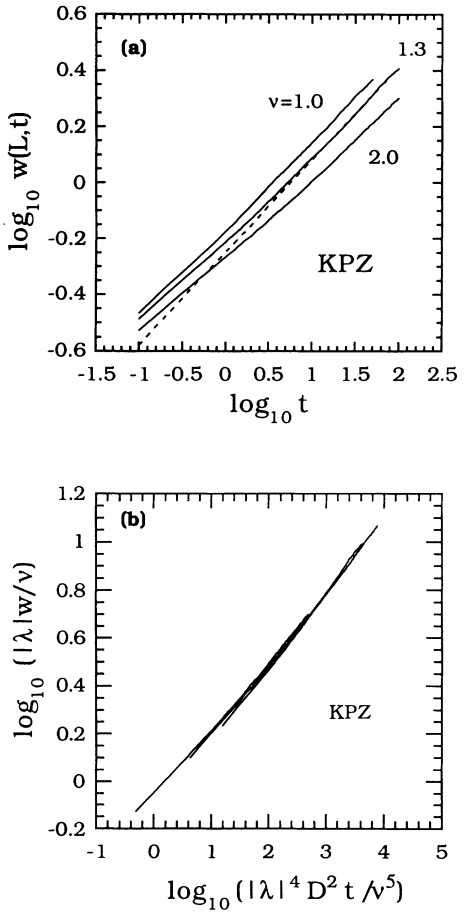

FIG. 13. (a) Log-log plot of $w(L,t)$ from numerical integration of KPZ equation ($D=0.5$, $\lambda=5.0$) and three different values of ν. Fits to late-time data (see dashed line) for $\nu=1.0$ and 1.3 have slopes close to $\frac{1}{3}$ (0.325 and 0.331) yielding values for the amplitude $C_t \simeq 0.66$ ($\nu=1.0$) and $C_t \simeq 0.56$ ($\nu=1.3$). (b) Scaling plot of data in (a) using Eq. (18).

likely because of the small system size.

In order to measure the coefficient u_t and the amplitude ratio R directly, as well as to test our general scaling relation Eq. (18), we also measured $w(L,t)$ at early times. In these simulations, the system size ($L=2^{18}$) was taken to be very large to avoid saturation effects, with $\Delta x=\frac{1}{2}$ and $\Delta t=0.005$. Figure 13(a) shows log-log plots of our raw data for the surface width $w(L,t)$ in $d=2$ for three different values of ν ($\nu=1.0$, 1.3, and 2.0) with $D=0.5$ and $\lambda=5$. We note that for $\nu=1.0$ and $\nu=1.3$ the data already show the expected $t^{1/3}$ behavior at late times. Figure 13(b) shows the same data scaled using the scaling form (18). The data scale reasonably well using this form. The small deviations observed are within the fluctuations and are essentially due to the difficulty of integrating the KPZ equation for long times accurately. From the measured values of C_t for $\nu=1.0$ and $\nu=1.3$, we obtain $u_t=C_t/[\lambda^{1/3}(D/\nu)^{2/3}]\simeq 0.61$, which is close to our mode-coupling-approximation prediction $u_t \simeq 0.71$. Combining the measured values of u_t and u_L, we obtain $R=u_t/u_L^{4/3}\simeq 3.2\pm 0.1$, which is in reasonable agreement with the value $R=3.45\pm 0.05$ obtained earlier from our discrete simulations.

V. DISCUSSION AND CONCLUSION

Using a scaling approach, we have derived expressions for the behavior of the asymptotic surface-width and correlation-function amplitudes as a function of macroscopic parameters for several different surface-growth models. From these expressions, we predicted a variety of universal amplitude ratios as well as universal scaling functions for these equations. We note that, in contrast to the type of scaling arguments used to predict exponents (which involve estimating the scaling behavior of fluctuating quantities over different length scales) our scaling analysis is exact. The only implicit assumption is that there are no additional length scales, such as small-length-scale cutoffs, which (while not present in the continuum equations) become important in the analysis of discrete models.

In particular, we assumed that the noise correlations were of the form $\langle \eta(\mathbf{x},t)\eta(\mathbf{x}',t')\rangle=\delta^{d-1}(\mathbf{x}-\mathbf{x}')\delta(t-t')$, with no short-length-scale cutoff on the δ functions. For some models, such as the KPZ equation for $d>3$ for which a phase transition is known to occur [3,16,17], this may not be the case. One example is the problem of a one-dimensional interface with surface tension ν, which is roughened by quenched random impurities of strength Δ at a temperature T. For this problem, the equal-time correlation function amplitude (A_x) has been shown [40] to depend on a transverse cutoff length ($a_\perp$) as well as the macroscopic parameters T, ν, and Δ. In this case, however, a scaling analysis similar to ours, but which takes into account the short-length cutoff, may still be performed.

In the case of the KPZ equation in $d=2$, however, our assumption that the short-length-scale cutoff is irrelevant in the asymptotic limit is justified by the fact that our mode-coupling approximation yielded the same scaling form as obtained from our scaling analysis. In particular,

our mode-coupling analysis indicated that the growth coefficients, as well as the steady-state coefficients and amplitude ratios R and R_G, are independent of cutoffs in the asymptotic limit and thus are truly universal. In addition, our simulation results appear to confirm this result. In the case of the other surface-growth models we have analyzed (Secs. II D and II E), we expect this assumption also to hold for $d \leq d_c$, since a similar scaling analysis [42] predicts correctly the growth exponents for these models. We note that results similar to ours for the KPZ equation have also been obtained by Hwa and Frey [41] for the correlation function $G(x,t)$, using a self-consistent mode-coupling analysis, which they claim is exact. The value of R_G predicted (0.69) is consistent with our simulations.

We now summarize our results for the KPZ equation in $d=2$. From simulations of two different discrete models we have confirmed the existence of a universal scaling function of the form of Eq. (22a). In addition, from simulations of three different discrete models for several values of the driving force f, we have determined the surface width amplitude ratio $R \simeq 3.45 \pm 0.05$, the correlation function amplitude ratio $R_G \simeq 0.71$, and the velocity scaling amplitude ratio $R_V \simeq 6.5 \pm 0.1$. We note that our results for R_V are somewhat higher than expected on the basis of known results which imply $R_V = 6.0$ for the single-step model. However, we have shown that this is most likely due to crossover effects. Our results for R may be compared with recent work by Krug, Meakin, and Halpin-Healy [28] who measured the universal amplitude ratio $c_2 = [C_t^2/(|\lambda| A_x^2)^{2/3}] = u_t^2/g_x^{4/3} \simeq 0.40$. Since $g_x = 1$ this implies $R = \sqrt{c_2}/u_L^{4/3} \simeq 3.3$ in reasonable agreement with our results. Our results for R imply that for the experimentally measurable case of free boundary conditions, $R^f = R/2^{2/3} \simeq 2.1$.

In addition to our simulations, we have also carried out a mode-coupling-approximation calculation using the first-order renormalization-group equations. From this calculation we confirmed the scaling forms predicted by our scaling analysis and found reasonable agreement with our simulation results, finding in particular $u_t \simeq 0.71$, $R \simeq 3.7$, and $R_G = g_t \simeq 0.63$. In addition, we found very good agreement with our simulation results for the scaling function $F(x)$ with periodic boundary conditions. From our mode-coupling calculation we also confirmed that the steady-state coefficients are the same as for the linear ($\lambda = 0$) case, for which we found $u_L = 1/\sqrt{12}$, $u_L^f = 1/\sqrt{6}$, and $g_x = 1$.

We have also determined the universal constants and amplitude ratios from direct integration of the KPZ equation in $d=2$, from which we obtained $R = 3.2 \pm 0.1$ and $u_t \simeq 0.61$, in reasonable agreement with our simulation results, as well as obtaining good agreement for the steady-state coefficients u_L and g_x. Good agreement with our general scaling form (18) from simulations for different values of ν was also obtained. One problem that still remains is an exact analytical determination of the universal coefficients u_t and g_t. Similarly, it would be interesting to know if there is a simple relation between R and R_G, or if these two quantities are essentially independent universal constants.

The results obtained here should be useful in establishing a more quantitative connection between the KPZ equation and various discrete growth models. In addition, we expect that the scaling analysis employed here should be useful in the analysis of experiments and in the study of a variety of other models of surface growth. The concept of universal amplitude ratios and scaling functions is one which will most likely be applied rather generally to both experiments and models in the future. In particular it is interesting to speculate that Eqs. (18)–(26) might also hold in the case of the Zhang model [36] of surface growth, which is a generalization of the (discrete) KPZ equation to include a power-law distribution in the noise amplitude [$P(\eta) = 1/\eta^{\mu+1}$]. For this model, μ-dependent exponents have been observed in both $d=2$ and 3 [35–37,43,44]. In $d=2$ it has been suggested as an explanation for recent experiments on flow in porous media [29,30]. However, the application of our scaling ideas in this case is not entirely certain, since it has been argued [45] that the Zhang model does not correspond properly to a continuum form of Eq. (2).

ACKNOWLEDGMENTS

This work was supported by the U.S. Office of Naval Research and the Petroleum Research Fund Administered by the American Chemical Society.

APPENDIX

In this appendix we derive Eqs. (40) and (53) for the surface width $w^2(L,t)$ and correlation function $G(x,t)$ in the linear ($\lambda = 0$) case, which are the starting point of the mode-coupling calculation.

1. Calculation of surface width $w(L,t)$

Performing the Fourier transform $\hat{h}(k,t) = (1/2\pi)\int_{-\infty}^{\infty} dx\, e^{-ikx} h(x)$, the Edwards-Wilkinson equation becomes

$$\frac{\partial \hat{h}}{\partial t} = -\nu k^2 \hat{h} + \hat{\eta}(k,t) , \tag{A1a}$$

where

$$\langle \hat{\eta}(k,t)\hat{\eta}(k',t') \rangle = \frac{D}{\pi}\delta(k+k')\delta(t-t') . \tag{A1b}$$

The solution of (A1) may be written as

$$\hat{h}(k,t) = \int_0^t ds\, \hat{\eta}(k,s) e^{-\nu k^2 (t-s)} \tag{A2}$$

assuming a flat interface [$h(x,0)=0$] at $t=0$. The width squared w^2 is then given by

$$w^2 = \langle h(x,t)^2 \rangle = \left\langle \int_{-\infty}^{\infty} dk\, e^{ikx} \hat{h}(k,t) \int_{-\infty}^{\infty} dk' e^{ik'x} \hat{h}(k',t') \right\rangle . \tag{A3}$$

Substituting (A2) into (A3), and taking into account Eq. (A1b), we obtain

$$w^2=\frac{D}{\pi}\int_{-\infty}^{\infty}dk\int_0^t ds\, e^{-2\nu k^2(t-s)}$$
$$=\frac{D}{2\pi\nu}\int_{-\infty}^{\infty}dk\frac{1}{k^2}(1-e^{-2\nu k^2 t}) . \quad \text{(A4)}$$

Putting in cutoffs $\Lambda_L\sim 1/L$ and $\Lambda_a\sim 1/a$ due to the system size L and the lower length cutoff a, we obtain

$$w^2(L,t)=\frac{D}{\pi\nu}\int_{\Lambda_L}^{\Lambda_a}dk\frac{1}{k^2}(1-e^{-2\nu k^2 t}) . \quad \text{(A5)}$$

2. Calculation of u_L^f for free boundary conditions

We would like to calculate the quantity $w_f(L,\infty)$, where $w_f(L,\infty)$ is the surface width at saturation in a region of size L embedded in a much larger system of size N. By definition we have

$$w_f^2(L,t)=\left\langle\frac{1}{L}\int_0^L h^2(x,t)dx\right\rangle-\left\langle\frac{1}{L^2}\left[\int_0^L h(x,t)dx\right]^2\right\rangle . \quad \text{(A6)}$$

Substituting for $h(x,t)$ its Fourier transform as above and using Eqs. (A1b) and (A2), this may be rewritten,

$$w_f^2(L,t)=\frac{2D}{\pi\nu L^2}\int_{\Lambda_N}^{\Lambda_a}dk\frac{1}{k^4}[(kL)^2/2-1+\cos(kL)]\times(1-e^{-2\nu k^2 t}) , \quad \text{(A7)}$$

where $\Lambda_a\sim 1/a$ and $\Lambda_N\sim 1/N$. In the $t\to\infty$ (saturation) limit, this becomes (taking $u=kL$, $L/a\gg 1$, and $L/N\to 0$)

$$w_f^2(L,\infty)=\frac{2DL}{\pi\nu}\int_0^\infty du\frac{1}{u^4}[u^2/2-1+\cos(u)]=\frac{D}{6\nu}L \quad \text{(A8)}$$

which implies $u_L^f=1/\sqrt{6}$.

This result may also be obtained from an analysis of the single-step model as follows. For the single-step model, it may be shown [34] that at saturation the interface is a random walk of up ($\sigma_i=+1$) and down ($\sigma_i=-1$) steps. For a given walk (realization of $\{\sigma_i\}$), $\langle h\rangle_L=1/L\sum_1^L h_i$, where $h_i=\sum_{l=1}^i\sigma_l$, which implies

$$\langle h\rangle_L=\frac{1}{L}\sum_{i=1}^{L}(L-i+1)\sigma_i$$

and

$$\langle h^2\rangle_L=\frac{1}{L}\sum_{i=1}^{L}h_i^2=\frac{1}{L}\sum_{i=1}^{L}\left[\sum_{l=1}^{i}\sigma_l\right]^2 .$$

Averaging over all realizations of σ_i, we obtain $\langle\langle h^2\rangle_L\rangle_\sigma=1/L\sum_1^L i=L/2$ for large L, and

$$\langle(\langle h\rangle_L)^2\rangle_\sigma=\frac{1}{L^2}\sum_1^L(L-i+1)^2=L/3$$

for large L. Subtracting we obtain $w_f^2(L,\infty)=L/6$, which implies $C_L^f=1/\sqrt{6}$. For the single-step model, $D/\nu=1$ since for periodic boundary conditions, $C_L=1/\sqrt{12}$ and $u_L=1/\sqrt{12}$. (This is also consistent with $A_x=D/\nu=\sum_{i=1}^L\langle\sigma_i^2\rangle/L=1$.) Thus, $u_L^f=C_L^f/\sqrt{D/\nu}=1/\sqrt{6}$.

3. Calculation of $G(x,t)$ for Edwards-Wilkinson equation

We first note that one may write $G(x,t)=2C(0,0)-2C(x,t)$, where $C(x,t)=\langle\tilde h(x+x',t+t')\tilde h(x',t')\rangle$ and $\tilde h(x,t)=h(x,t)-\langle h(x,t)\rangle_x$. For the case $\lambda=0$, $\langle h(x,t)\rangle_x=0$ so that in terms of the Fourier transform $\tilde h(k,t)$ one may write

$$C(x,t)=\left\langle\int_{-\infty}^{\infty}dk\, e^{ik(x+x')}\hat h(k,t+t')\int_{-\infty}^{\infty}dk'\, e^{ik'x'}\hat h(k',t')\right\rangle . \quad \text{(A9)}$$

Substituting Eq. (A2) as before this becomes

$$C(x,t)=\int_{-\infty}^{\infty}dk\, e^{ik(x+x')}\int_0^{t+t'}ds\,\hat h(k,s)e^{-\nu k^2(t+t'-s)}\int_{-\infty}^{\infty}dk'\, e^{ik'x'}\int_0^{t'}ds'\,\hat h(k',s')e^{-\nu k'^2(t'-s')} . \quad \text{(A10)}$$

Taking into account Eq. (A1b) we obtain

$$C(x,t)=e^{-\nu k^2(t+2t')}\frac{D}{\pi}\int_{-\infty}^{\infty}dk\, e^{ikx}\int_0^{t+t'}ds\, e^{\nu k^2 s}\int_0^{t'}ds'\, e^{\nu k^2 s'}\delta(s-s')$$
$$=e^{-\nu k^2(t+2t')}\frac{D}{\pi}\int_{-\infty}^{\infty}dk\, e^{ikx}\int_-^+ d(\Delta s)\delta(\Delta s)\int_0^{t'}dS\, e^{2\nu k^2 S} , \quad \text{(A11)}$$
$$C(x,t)=\frac{D}{2\pi\nu}\int_{-\infty}^{\infty}dk\frac{1}{k^2}e^{ikx}(e^{-\nu k^2 t}-e^{-\nu k^2(t+2t')}) ,$$

where $\Delta s=s-s'$ and $S=(s+s')/2$. In the saturation limit ($t'\gg L^z$) this becomes

$$C(x,t)=\frac{D}{2\pi\nu}\int_{-\infty}^{\infty}dk\frac{1}{k^2}e^{ikx}e^{-\nu k^2 t} \quad \text{(A12)}$$

so that

$$G(x,t)=2C(0,0)-2C(x,t)$$
$$=\frac{2D}{\pi\nu}\int_0^\infty dk\frac{1}{k^2}[1-\cos(kx)e^{-\nu k^2 t}]\ . \tag{A13}$$

Putting in the appropriate cutoffs, we obtain Eq. (56).

[1] *Dynamics of Fractal Surfaces,* edited by F. Family and T. Vicsek (World-Scientific, Singapore, 1991).
[2] F. Family and T. Vicsek, J. Phys. A **18**, L75 (1985).
[3] M. Kardar, G. Parisi, and Y.-C. Zhang, Phys. Rev. Lett. **56**, 889 (1986).
[4] D. Forster, D. R. Nelson, and M. J. Stephen, Phys. Rev. A **16**, 732 (1977).
[5] S. F. Edwards and D. R. Wilkinson, Proc. R. Soc. London Ser. A **381**, 17 (1982).
[6] R. Jullien and R. Botet, J. Phys. A **18**, 2279 (1985).
[7] P. Meakin, P. Ramanlal, L. M. Sander, and R. C. Ball, Phys. Rev. A **34**, 5091 (1986).
[8] J. Kertész and D. E. Wolf, J. Phys. A **21**, 747 (1988).
[9] J. M. Kim and J. M. Kosterlitz, Phys. Rev. Lett. **62**, 2289 (1989).
[10] A. De Masi, P. A. Ferrari, and M. E. Vares, J. Stat. Phys. **55**, 601 (1989).
[11] In Ref. [10] it is shown that in the steady-state limit the single-step model may be mapped onto the *stationary* Burgers equation. However, no discussion of the dynamical behavior is given.
[12] J. G. Amar and F. Family, Phys. Rev. A **45**, 3373 (1992).
[13] L.-H. Tang, T. Nattermann, and B. M. Forrest, Phys. Rev. Lett. **65**, 2422 (1990).
[14] T. Sun, H. Guo, and M. Grant, Phys. Rev. A **40**, 6763 (1989).
[15] Z. W. Lai and S. Das Sarma, Phys. Rev. Lett. **66**, 2348 (1991).
[16] B. M. Forrest and L.-H. Tang, Phys. Rev. Lett. **64**, 1504 (1990).
[17] H. Yan, D. Kessler, and L. M. Sander, Phys. Rev. Lett. **64**, 926 (1990); Y. P. Pellegrini and R. Jullien, Phys. Rev. Lett. **64**, 1745 (1990).
[18] E. Medina, T. Hwa, M. Kardar, and Y.-C. Zhang, Phys. Rev. A **39**, 3053 (1989).
[19] D. E. Wolf and L.-H. Tang, Phys. Rev. Lett. **65**, 1591 (1990).
[20] D. A. Huse, C. L. Henley, and D. S. Fisher, Phys. Rev. Lett. **55**, 2924 (1985).
[21] J. Krug and P. Meakin, J. Phys. A **23**, L987 (1990).
[22] M. Plischke, Z. Racz, and D. Liu, Phys. Rev. B **35**, 3485 (1987).
[23] J. W. Evans and H. C. Kang, J. Math. Phys. **32**, 2918 (1991).
[24] In Ref. [21], the value of λ for the single-step model is incorrectly given as $-\frac{1}{2}$.
[25] J. G. Amar and F. Family, Phys. Rev. A **41**, 3399 (1990).
[26] K. Kawasaki, in *Phase Transitions and Critical Phenomena,* edited by C. Domb and M. S. Green (Academic, London, 1976), Vol. 5a.
[27] K. Kawasaki and J. D. Gunton, Phys. Rev. B **13**, 4658 (1976).
[28] J. Krug, P. Meakin, and T. Halpin-Healy, Phys. Rev. A **45**, 638 (1992).
[29] M. A. Rubio, C. A. Edwards, A. Dougherty, and J. P. Gollub, Phys. Rev. Lett. **63**, 1685 (1989).
[30] V. K. Horváth, F. Family, and T. Vicsek, Phys. Rev. Lett. **65**, 1388 (1990); V. K. Horváth, F. Family, and T. Vicsek, J. Phys. A **24**, L25 (1991); Phys. Rev. Lett. **67**, 3207 (1991).
[31] N. Martys, M. Cieplak, and M. O. Robbins, Phys. Rev. Lett. **66**, 1058 (1991).
[32] D. A. Huse, J. G. Amar, and F. Family, Phys. Rev. A **41**, 7075 (1990).
[33] Because of the reasonably large intrinsic width of the ballistic deposition model, the value of C_L obtained depended somewhat on the type of fit used [$w(L,\infty)$ versus $L^{1/2}$ or $w^2(L,\infty)$ versus L]. The value we used was obtained from a linear fit of the form $w^2(L,\infty)$ versus L ($L=16-512$), from which we obtained $C_L^2\simeq 0.049$ or $C_L\simeq 0.22$.
[34] L. M. Sander and H. Yan, Phys. Rev. A **44**, 4885 (1991).
[35] J. G. Amar and F. Family, J. Phys. I (Paris) **1**, 175 (1991); J. G. Amar and F. Family (unpublished).
[36] Y.-C. Zhang, J. Phys. (Paris) **51**, 2129 (1990).
[37] J. G. Amar and F. Family, J. Phys. A **24**, L79 (1991).
[38] J. M. Kim, M. A. Moore, and A. J. Bray, Phys. Rev. A **44**, 2345 (1991).
[39] Using a similar integration scheme in $d=3$ (see Ref. [25]) we have also obtained good agreement with the known results for the linear model: $w^2(L,\infty)=(D/2\pi\nu)\ln L$ and $w^2(\infty,t)=(D/4\pi\nu)\ln t$.
[40] T. Nattermann and W. Renz, Phys. Rev. B **38**, 5182 (1988).
[41] T. Hwa and E. Frey, Phys. Rev. A **44**, 7873 (1991).
[42] H. G. E. Hentschel and F. Family, Phys. Rev. Lett. **66**, 1982 (1991).
[43] S. V. Buldyrev, S. Havlin, J. Kertesz, H. E. Stanley, and T. Vicsek, Phys. Rev. A **43**, 7113 (1991).
[44] R. Bourbonnais, J. Kertesz, and D. E. Wolf, J. Phys. II (Paris) **1**, 495 (1991).
[45] Y.-C. Zhang, Physica A **170**, 1 (1990).